

***GW* study of the metal-insulator transition of bcc hydrogen**

Je-Luen Li, G.-M. Rignanese,* Eric K. Chang, Xavier Blase,† and Steven G. Louie

*Department of Physics, University of California at Berkeley, Berkeley, California 94720**and Materials Sciences Division, Lawrence Berkeley National Laboratory, Berkeley, California 94720*

(Received 4 February 2002; published 1 July 2002)

We study the metal-insulator transition in a model Mott system, a bcc hydrogen solid, by performing *ab initio* quasiparticle band-structure calculations within the *GW* approximation for a wide range of lattice constants. The value of the critical electron density n_c is consistent with Mott's original criterion. For smaller lattice constants, our spin-polarized *GW* results agree well with previous variational quantum Monte Carlo calculations. For large lattice constants, the computed quasiparticle band gap corresponds to the difference between the ionization energy and electron affinity of an isolated hydrogen atom. Near the metal-insulator transition, we investigate the quality of the quasiparticle wave functions obtained from different starting approximations in density-functional theory. Finally, we gain new insight into the *GW* method and its applicability to spin-polarized systems, for which several refinements are introduced.

DOI: 10.1103/PhysRevB.66.035102

PACS number(s): 71.30.+h, 71.45.Gm

I. INTRODUCTION

A metal-insulator transition induced by a correlation effect is an old problem in condensed-matter physics. Mott¹ first described this kind of transition by considering a crystalline array of hydrogenlike atoms. Depending on the separations between neighboring atoms, the material is metallic (small lattice constant) or insulating (large lattice constant). Mott discussed the transition based on a screening argument, and concluded that the transition is first order. Together with a number of approximations, a simple criterion for the critical electron density n_c at the transition was derived,

$$n_c^{1/3} a_0^* \approx 0.26,$$

where

$$a_0^* = \frac{\kappa \hbar^2}{e^2 m^*},$$

κ is the static dielectric constant, and m^* is the effective mass of the electron in the crystal. This equation is in satisfactory agreement for a range of doped semiconductors;^{2,3} however, the transition for these systems may be of Mott or Anderson type depending on the doping conditions. For $\kappa = 1$ and $m^* = m_e$, the transition occurs at a Wigner-Seitz radius $r_s \approx 2.39$ a.u.

Following Mott's seminal work and the development of modern electronic structure calculation, several groups applied *ab initio* methods to compute the band gap of a crystalline atomic hydrogen solid as a function of r_s within the density functional theory (DFT). Early studies based on the local spin density approximation (LSDA) (Refs. 4–7) supported a second-order transition picture. Two transitions, a paramagnetic-antiferromagnetic (PM-AFM) transition in the metallic phase and a metal-insulator transition, were found to occur at $r_s = 2.55$ and 2.85 a.u. respectively.⁷ Svane and Gunnarsson⁸ used a self-interaction-corrected (SIC) LSDA and found a simultaneous first order PM-AFM and metal-insulator transition at $r_s = 2.45$ a.u. Recently, using the gen-

eralized gradient approximation (GGA) with DFT, Pfrommer *et al.*⁹ obtained a PM-AFM transition at $r_s = 2.25$ a.u. and a metal-insulator transition at $r_s = 2.50$ a.u.

Although it is suspected that the metallic solid form of atomic hydrogen is an important constituent of the core of the large planets, it is still unrealizable in the laboratory with present day high-pressure techniques. Thus we can only rely on calculations such as those performed using the variational quantum Monte Carlo (VQMC) method to compare with our present study. For example, Zhu¹⁰ reported a PM-AFM transition at $r_s = 2.2$ a.u. and a metal-insulator transition at $r_s = 2.2 - 2.3$ a.u. from his VQMC studies. However, the statistical noise in those calculations is too large to discriminate between a weak first-order transition or a second-order transition. Furthermore, since the VQMC method is a computationally demanding method, these calculations have been restricted to small values of r_s (up to 4 a.u.) and small supercells.

In this paper, we report *ab initio* quasiparticle (QP) band-structure calculations in the *GW* approximation for bcc atomic hydrogen. This many-body Green's-function approach is known to be quite accurate for a wide variety of bulk insulators.^{11,12} It is also computationally more efficient than the VQMC method, so we are able to extend the study over a broader range of lattice constants. This allows us to obtain results in the dilute limit where the hydrogen atoms are isolated and compare to atomic data.

We also address in this paper several theoretical issues. First the *GW* formalism is generalized to treat spin-polarized systems¹³ in a plane wave basis set. Second, we demonstrate the necessity to account for the off-diagonal elements of the self-energy operator evaluated in the DFT eigenstate basis (i.e., mixing of different DFT eigenstates in determining the QP wave functions). Our calculations provide further insight into the "orbital stability" problem, i.e., the closeness between QP wave functions and DFT eigenfunctions.

II. SPIN-POLARIZED *GW* APPROXIMATION

In this section, we present the formalism used to compute the quasiparticle energies and wave functions of spin-

polarized systems. A rigorous formulation for the quasiparticle properties is based on Green's function approach.^{11,14} The quasiparticle energies $E_{n,k}^{QP}$ and wave functions $\psi_{n,k}^{QP}$ are obtained by solving the equation

$$(T + V_{ext} + V_H) \psi_{n\sigma k}^{QP}(\mathbf{r}) + \sum_{\sigma'} \int \Sigma^{\sigma\sigma'}(\mathbf{r}, \mathbf{r}', E_{n\sigma k}) \psi_{n\sigma'k}^{QP}(\mathbf{r}') d\mathbf{r}' = E_{n\sigma k} \psi_{n\sigma k}^{QP}(\mathbf{r}), \quad (1)$$

where the spin index σ has been explicitly labeled in addition to band indices n and wave vectors \mathbf{k} . T is the kinetic energy operator, V_{ext} is the external potential due to the ions, and V_H is the Hartree potential. In this equation, the exchange and correlation effects are described by the electron self-energy operator $\Sigma^{\sigma\sigma'}(\mathbf{r}, \mathbf{r}', E_{n\sigma k})$, which is nonlocal and energy dependent. The real part of $E_{n\sigma k}$ is the energy of the quasiparticle $E_{n\sigma k}^{QP}$, while the imaginary part gives its lifetime.

In the following, we *assume* that there is no spin-flip when an electron is propagating in the system. As a consequence, the one-particle Green's function $G^{\sigma\sigma'}(\mathbf{r}, \mathbf{r}'; \omega)$ and

the self-energy operator $\Sigma^{\sigma\sigma'}(\mathbf{r}, \mathbf{r}', E_{n\sigma k})$ are diagonal in spin space. Equation (1) thus decouples into

$$(T + V_{ext} + V_H) \psi_{n\sigma k}^{QP}(\mathbf{r}) + \int \Sigma^{\sigma\sigma}(\mathbf{r}, \mathbf{r}', E_{n\sigma k}) \psi_{n\sigma k}^{QP}(\mathbf{r}') d\mathbf{r}' = E_{n\sigma k} \psi_{n\sigma k}^{QP}(\mathbf{r}). \quad (2)$$

Within the GW approximation, the self-energy operator is given by

$$\Sigma^{\sigma\sigma}(\mathbf{r}, \mathbf{r}', \omega) = \frac{i}{2\pi} \int G^{\sigma\sigma}(\mathbf{r}, \mathbf{r}', \omega - \omega') W(\mathbf{r}, \mathbf{r}', \omega') e^{-i\delta\omega'} d\omega'. \quad (3)$$

The screened Coulomb interaction W is

$$W_{G,G'}(\mathbf{q}, \omega) = \epsilon_{G,G'}^{-1}(\mathbf{q}, \omega) V(\mathbf{q} + \mathbf{G}'), \quad (4)$$

where $V(\mathbf{q} + \mathbf{G})$ is the bare Coulomb interaction $4\pi/|\mathbf{q} + \mathbf{G}|^2$ expressed in Fourier space.

Within the random phase approximation (RPA), the static polarizability is evaluated in DFT and is also diagonal in the spin dimension:

$$P_{G,G'}^{\sigma\sigma'}(\mathbf{q}, \omega=0) = \delta_{\sigma,\sigma'} \sum_{nn'k} \frac{\langle n\sigma, \mathbf{k} | e^{-i(\mathbf{q}+\mathbf{G})\cdot\mathbf{r}} | n'\sigma, \mathbf{k}-\mathbf{q} \rangle \langle n'\sigma, \mathbf{k}-\mathbf{q} | e^{i(\mathbf{q}+\mathbf{G}')\cdot\mathbf{r}'} | n\sigma, \mathbf{k} \rangle}{E_{n'\sigma k-\mathbf{q}}^{DFT} - E_{n\sigma k}^{DFT}}. \quad (5)$$

Here the index n runs over all occupied states, and n' over all unoccupied states. In terms of the polarizability, the inverse of the static dielectric function $\epsilon_{G,G'}^{-1}(\mathbf{q}, \omega=0)$ is given by the matrix inversion of

$$\epsilon_{G,G'}(\mathbf{q}, \omega=0) = \delta_{G,G'} - V(\mathbf{q} + \mathbf{G}) [P_{G,G'}^{\uparrow\uparrow}(\mathbf{q}, \omega=0) + P_{G,G'}^{\downarrow\downarrow}(\mathbf{q}, \omega=0)], \quad (6)$$

so that the local field corrections are included. To compute the dielectric function at finite, nonzero frequencies, we make use of a generalized plasmon-pole model as discussed in Ref. 11.

When one tries to solve the quasiparticle equation (2), usually the first step is to take quasiparticle wave functions from the DFT or Hartree-Fock theory. We may expand $\psi_{n\sigma k}^{QP}$ in DFT eigenfunctions:

$$\psi_{n\sigma k}^{QP} = \sum_m \alpha_{nm\sigma k} \phi_{m\sigma k}^{DFT}. \quad (7)$$

In this basis set, Eq. (2) can be expressed as a matrix eigenvalue equation and one faces the task of diagonalizing the self-energy operator $\langle \phi_{nk}^{DFT} | \Sigma | \phi_{mk}^{DFT} \rangle$. Alternatively, we can treat $\Sigma(E) - V_{xc}$ as a perturbation term where V_{xc} is the exchange correlation potential in the Kohn-Sham equation.

Assuming that $\Sigma(E)$ is a slowly varying function of E , a second order perturbation calculation gives rise to an explicit formula for $E_{n\sigma k}^{QP}$:

$$E_{n\sigma k}^{QP} = E_{n\sigma k}^{DFT} + Z_{n\sigma k} \langle \phi_{n\sigma k}^{DFT} | \Sigma(E_{n\sigma k}^{DFT}) - V_{xc} | \phi_{n\sigma k}^{DFT} \rangle + \sum_{m \neq n} \frac{|\langle \phi_{m\sigma k}^{DFT} | \Sigma(E_{n\sigma k}^{DFT}) - V_{xc} | \phi_{n\sigma k}^{DFT} \rangle|^2}{E_{n\sigma k}^{DFT} - E_{m\sigma k}^{DFT}}$$

where

$$Z_{n\sigma k} = \frac{1}{1 - \langle \phi_{n\sigma k}^{DFT} | d\Sigma_{n\sigma k}(E_{n\sigma k}^{DFT}) / dE_{n\sigma k}^{DFT} | \phi_{n\sigma k}^{DFT} \rangle}. \quad (8)$$

The coefficients $\alpha_{nm\sigma k}$ to first order are given by

$$\alpha_{nm\sigma k} = 1 \quad (n=m) \\ \alpha_{nm\sigma k} = \frac{\langle \phi_{m\sigma k}^{DFT} | \Sigma(E_{n\sigma k}^{DFT}) - V_{xc} | \phi_{n\sigma k}^{DFT} \rangle}{E_{n\sigma k}^{DFT} - E_{m\sigma k}^{DFT}} \quad (n \neq m). \quad (9)$$

The assumption $\alpha_{nm\sigma k} = \delta_{nm}$, namely, that the QP wave functions are identical to the DFT eigenfunctions, is often used since this assumption is found to lead to negligible errors in the quasiparticle energies in simple s - p bonded semiconductors.^{11,12} However, as is shown below, the QP

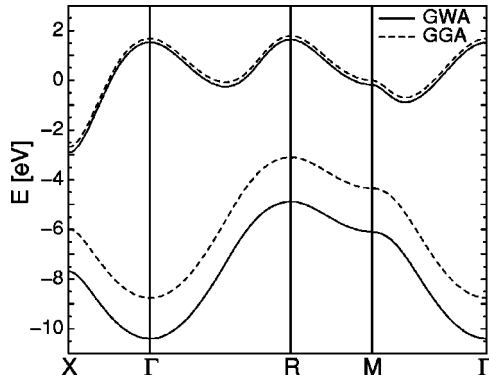


FIG. 1. Band structure of bcc hydrogen calculated in the GGA (dashed line) and the GW approximation (solid line) at $r_s = 2.6$ a.u.

wave functions can be different from the DFT eigenstates near the metal-insulator transition of bcc hydrogen. This difference has also been observed in other systems.^{15,16}

III. COMPUTATIONAL DETAILS

Our DFT calculations are performed using a local hydrogen pseudopotential of the Kerker type¹⁷ with a cutoff radius 0.7 a.u. The wave functions are expanded in plane waves up to an 85-Ry energy cutoff. For $r_s \geq 3.0$ a.u. a $4 \times 4 \times 4$ Monkhorst-Pack¹⁸ grid is used to sample the Brillouin zone, whereas for $r_s < 3.0$ a.u. the sampling has to be increased to an $8 \times 8 \times 8$ grid. These grids include 10 and 35 \mathbf{k} points in the irreducible wedge of the bcc Brillouin zone, respectively. For the LSDA calculation, we use the Ceperley-Alder¹⁹ exchange-correlation functional, and for the GGA calculation we make use of the PBE exchange-correlation functional.²⁰

In the GW calculation, we compute the static dielectric function $\epsilon_{G,G'}(\mathbf{q}, \omega=0)$ for \mathbf{G} vectors of kinetic energy up to 24 Ry. The self-energy operator Σ is obtained by summing over the Brillouin zone, and over 49 conduction bands. All of these cutoffs guarantee a numerical convergence of better than 0.1 eV in the quasiparticle energies.

IV. RESULTS AND DISCUSSION

We first obtain eigenfunctions and eigenvalues in the LSDA and the GGA. These are then used to construct the spin-polarized Green's functions in the GW approximation. A typical band structure in the antiferromagnetic insulating phase ($r_s = 2.6$) is shown in Fig. 1 where we compare the GGA and GW calculation. When the magnetic ordering is taken into account, the crystal has two atoms in a cubic unit cell where the spin polarizations of the center and the corner hydrogen are antiparallel. Note that bcc hydrogen has an indirect gap from R to X , which we simply refer to as a band gap in the following discussion. Now in Fig. 2 we show the variation of the band gap as a function of r_s , computed in the LSDA, the GGA, and the GW approximation. The two different GW results are based on taking the LSDA or GGA results as the zeroth-order approximation in constructing the self-energy operator. It is readily seen that the GGA band gap

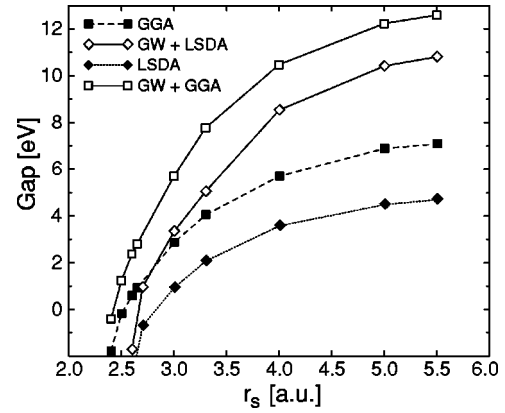


FIG. 2. The energy gap of AF bcc hydrogen as a function of the Wigner-Seitz radius r_s , computed in the LSDA (solid diamonds and dotted line), the GGA (solid squares and dashed line), and the GW approximation starting from either the LSDA (open diamonds and solid line) or GGA (open squares and solid line) results. The lines are guides to the eyes.

is systematically larger than the LSDA gap.⁹ The magnitude of the GW corrections to the band gap of bcc hydrogen is more dramatic when compared to the case of typical semiconductors. This is particularly true for large values of r_s , but note that, for small values of r_s , due to the steep slope of the curves near the metal-insulator transition, even a small change in the band gap yields a large difference of the critical electron density for the metal-insulator transition.

Figure 2 also shows that the quasiparticle band gap depends on the zeroth-order self-energy operator which is constructed from wave functions and dielectric functions obtained in either the LSDA or GGA. On the one hand, LSDA and GGA band gaps are different and therefore yield different dielectric functions within the RPA. At the charge density $r_s = 2.6$, the LSDA dielectric constant is $\epsilon(0) = 9.74$ and the GGA dielectric constant is $\epsilon(0) = 3.58$. On the other hand, LSDA and GGA wave functions have different degree of localization. To estimate the effect of these two slightly different wave functions, we compute the bare exchange term²¹ which depends solely on the wave functions:

$$\Sigma_x = - \sum_{n_1}^{\text{occ}} \sum_{\mathbf{q}, G, G'} \langle n\sigma\mathbf{k} | e^{i(\mathbf{q}+G)\cdot\mathbf{r}} | n_1\sigma, \mathbf{k}-\mathbf{q} \rangle \times \langle n_1\sigma, \mathbf{k}-\mathbf{q} | e^{-i(\mathbf{q}+G')\cdot\mathbf{r}'} | n\sigma\mathbf{k} \rangle V(\mathbf{q}+G'). \quad (10)$$

The difference in the value of this term between LSDA and GGA wave functions is about 1–2 eV for the bcc hydrogen system.

Since it is known that GGA wave functions are more localized and closer to the exact solution than the LSDA,⁹ and also that the GGA energies are closer to the quasiparticle spectrum, the RPA dielectric screening is better represented in the GGA than in the LSDA.²² Consequently, the GW self-energy corrections based on the GGA are more accurate than those based on the LSDA. For values of r_s near the metal-insulator transition, our GW results, based on the GGA, agree well with the VQMC calculation of Zhu,¹⁰ as shown in

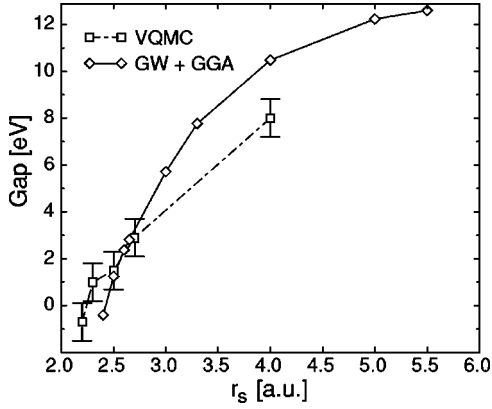


FIG. 3. The energy gap (in eV) of bcc hydrogen as a function of the Wigner-Seitz radius r_s (in a.u.), computed within the GW approximation (open diamonds and solid line) based on GGA results, and with the VQMC method (Ref. 10). Lines are guides to the eyes.

Fig. 3. The metal-insulator transition from the present study is predicted to occur at 2.42 a.u., in agreement with the result obtained with the SIC-LSDA method,⁸ and consistent with the VQMC prediction of 2.30 a.u.¹⁰ which has a significant error bar. For large values of r_s , our GGA+ GW band gap of 12.6 eV approaches the experimental value of 12.8 eV for isolated atomic hydrogens ($r_s \rightarrow \infty$). This is a noticeable improvement over results from the LSDA (4.7 eV), GGA (7.0 eV), and SIC-LSDA (10.9 eV).⁸ The GGA+ GW band gaps resemble the ones from the VQMC calculation for small lattice constants, but they differ significantly at $r_s=4$, the largest r_s value studied in Zhu's work. Being at the end of the data points, this value might have a larger statistical error. The overall trend of our band gaps indicates that at $r_s=5.5$ (equivalent to a 9.7-a.u. separation between nearest atoms), the wave functions of the neighboring hydrogen atoms have very little overlap. VQMC data would have suggested that one needs to go to larger values of r_s to attain the isolated hydrogen atom limit. A summary of previous studies regarding the charge density at the metal-insulator transition and the band gap in the atomic limit is shown in Table I.

At this point we would like to stress the significance of the off-diagonal elements $\langle m | \Sigma - V_{xc} | n \rangle$ expressed in the basis of DFT eigenfunctions. Contrary to what is commonly assumed in bulk semiconductors, they play a more important role in this system near the transition. As the distance between neighboring hydrogen atoms becomes smaller, there is more overlap between wave functions originating from nearby atomic sites and the energy bands become more dispersive. We can apply Eq. (9) to assess the difference between the DFT eigenfunctions and QP wave functions. It has been shown that for typical semiconductors like silicon, the overlap between the LDA and QP wave functions is better than 99.9%.¹¹ Near the metal-insulator transition density ($r_s=2.5$ a.u.), we found the mixing due to nonzero off-diagonal elements $\langle m | \Sigma - V_{xc} | n \rangle$ can be as large as 2.5% at the k -point X , while at other special k points they often vanish due to selection rules. It is found that these nonzero off-diagonal terms evaluated in the LSDA eigenfunction basis are larger than in the GGA eigenfunction basis. The GGA

TABLE I. Comparison of the results obtained in this study for the PM-AFM and metal-insulator transition point with those of previous studies of bcc hydrogen.

	r_s at the PM-AFM transition (a.u.)	r_s at the metal-insulator transition(a.u.)	Band gap for $r_s \rightarrow \infty$ (eV)
LSDA	2.50	2.78	4.7
GGA	2.25	2.50	7.0
LMTO-LSDA (Ref. 7)	2.55	2.85	
SIC-LSDA (Ref. 8)	2.45	2.45	10.9
GGA-PW91 (Ref. 9)	2.25	2.50	
VQMC (Ref. 10)	2.20	2.20–2.30	
LSDA+ GW	–	2.65	10.8
GGA+ GW	–	2.42	12.6
Expt.	–	–	12.8

wave functions are preferred based on this criterion. Although the second-order correction does not affect the band gap, it gives an indication as to which basis to choose from between LSDA and GGA wave functions when performing GW calculations.

We also studied the difference between GGA and QP wave functions. Using the perturbation scheme outlined in Eqs. (7)–(9), the off-diagonal elements are taken into account to expand quasiparticle wave functions in the DFT basis. For example, as discussed above, near the metal-insulator transition region ($r_s=2.5$ a.u.), the quasiparticle wave function for the first valence band at X is a linear combination of the GGA eigenfunctions:

$$\psi_{1,X}^{QP} = \phi_{1,X}^{GGA} + 0.025 \cdot \phi_{3,X}^{GGA}. \quad (11)$$

This 2.5% difference is much larger than the mixing in semiconductors. If we plot the square of the wave functions, the GGA wave-function peak is more pronounced while the quasiparticle wave function spreads out slightly over the region between the atomic sites of different spin. The contrast between GGA and QP wave functions is more obvious as r_s becomes smaller.

Under the assumption that the imaginary part of $E_{n\sigma k}$ is small, the charge density can be written as

$$\rho_{\sigma}(\mathbf{r}) = \sum_{n,k}^{\text{occ}} |\psi_{n\sigma k}^{QP}(\mathbf{r}, E_{n\sigma k})|^2 \quad (12)$$

where $E_{n\sigma k}$ is the energy allowed in the quasiparticle Eq. (2). The difference between QP and DFT charge densities is much less than that for the wave functions, because the density is related to the square of the wave functions. At the same condition given by Eq. (11), the mixing coefficient for the charge density is less than 0.1%. On more general grounds, within the Kohn-Sham formulation of DFT, the

charge density is exact while the single-particle eigenstates do not have a formal direct connection to the quasiparticle wave functions. As a result, there is no significant difference between DFT and GW charge densities. The PM-AFM transition point is found to be the same within the DFT and the GW approximation (see Table I).

V. CONCLUSION

In this paper, we have formulated and implemented the GW approximation for spin-polarized systems employing a plane-wave basis. Within this formalism, we have calculated the quasiparticle band structure of bcc hydrogen for r_s ranging from 2.4 a.u. (near the metal-insulator transition) to 5.5 a.u. (approaching the isolated atomic limit). The metal-insulator transition point is found to be very close to both VQMC and SIC-LSDA results, and for large values of r_s , the band gap correctly approaches the experimental value. We found a difference in the band gap calculated by LSDA + GW and GGA + GW methods, and concluded that the GGA + GW method is in better agreement with VQMC and experiment. The difference is attributable to the LSDA and GGA energy spectrum. The GGA eigenfunctions and eigenvalues are closer to the quasiparticle calculation results. We have also discussed the effect of the off-diagonal elements of

the $\Sigma - V_{xc}$ (when expressed in the DFT eigenstate basis) to the quasiparticle energy, wave function, and charge density. This effect is more pronounced near the metal-insulator transition region. We have shown, in particular, that the quasiparticle wave function at the top of the valence band can be expanded as a linear superposition of the DFT valence and conduction wave functions, and that the mixing of valence character causes the quasiparticle wave function to be different from the corresponding LSDA or GGA eigenfunctions. Finally, the charge density from the GW calculation is found to be almost identical to the DFT results.

ACKNOWLEDGMENTS

The authors would like to thank M. Rohlfing for discussions on the GW formalism for spin-polarized systems, and Young-Gui Yoon for enlightening discussions and assistance in the GGA calculations. This work was supported by the NSF under Grant No. DMR0087088, and by the Office of Energy Research, Office of Basic Energy Sciences, Materials Sciences Division of the U.S. Department of Energy under Contract No. DE-AC03-76SF00098. Computer time was provided by the NSF at the National Center for Supercomputing Applications and by the DOE at the Lawrence Berkeley National Laboratory's NERSC center.

*Present address: Unité de Physico-Chimie et de Physique des Matériaux, Université Catholique de Louvain, 1 Place Croix du Sud, B-1348 Louvain-la-Neuve, Belgium.

†Université Claude Bernard-Lyon I, Département de Physique des Matériaux and CNRS, 43, Bd du 11 Novembre 1918, 69622 Villeurbanne, France.

¹N. F. Mott, Proc. Phys. Soc. London **62**, 416 (1949).

²P. P. Edwards and M. J. Sienko, Phys. Rev. B **17**, 2575 (1978).

³N. F. Mott, *Metal-Insulator Transitions*, 2nd ed. (Taylor and Francis, London, 1990).

⁴A. Ghazali and P. Leroux Hugon, Phys. Rev. Lett. **41**, 1569 (1978).

⁵J. H. Rose, H. B. Shore, and L. M. Sander, Phys. Rev. B **21**, 3037 (1980).

⁶L. M. Sander, H. B. Shore, and J. H. Rose, Phys. Rev. B **24**, 4879 (1981).

⁷B. I. Min, T. Oguchi, H. J. F. Jansen, and A. J. Freeman, Phys. Rev. B **33**, 324 (1986).

⁸A. Svane and O. Gunnarsson, Solid State Commun. **76**, 851 (1990).

⁹B. G. Pfrommer and S. G. Louie, Phys. Rev. B **58**, 12 680 (1998).

¹⁰J. Zhu, Ph.D. thesis, University of California at Berkeley, 1990.

¹¹M. S. Hybertsen and S. G. Louie, Phys. Rev. B **34**, 5390 (1986).

¹²R. W. Godby, M. Schlüter, and L. J. Sham, Phys. Rev. B **37**, 10 159 (1988).

¹³F. Aryasetiawan, Phys. Rev. B **46**, 13 051 (1992).

¹⁴L. Hedin and S. Lundqvist, Solid State Phys. **23**, 1 (1969).

¹⁵O. Pulci, F. Bechstedt, G. Onida, R. Del Sole, and L. Reining, Phys. Rev. B **60**, 16 758 (1999).

¹⁶J. C. Grossman, M. Rohlfing, L. Mitas, S. G. Louie, and M. L. Cohen, Phys. Rev. Lett. **86**, 472 (2001).

¹⁷K. Ho, C. Elsässer, C. Chan, and M. Fähnle, J. Phys.: Condens. Matter **4**, 5189 (1992).

¹⁸H. J. Monkhorst and J. D. Pack, Phys. Rev. B **13**, 5188 (1976).

¹⁹D. M. Ceperley and B. J. Alder, Phys. Rev. Lett. **45**, 566 (1980).

²⁰J. P. Perdew, K. Burke, and M. Ernzerhof, Phys. Rev. Lett. **77**, 3865 (1996).

²¹See Eq. (34a) in Ref. 11.

²²In general, it is found that the GGA is a better approximation than the local-density approximation for the electronic properties of weakly bonded systems within density-functional theory.